International Journal of Modern Manufacturing Technologies
ISSN 2067–3604, Vol. XIV, No. 1 / 2022
https://doi.org/10.54684/ijmmt.2022.14.1.113

STRUCTURES OF GRADIENT LAYERS OBTAINED USING THE LASER METAL DEPOSITION (LMD) METHOD

Michał Urbańczyk[1], Janusz Adamiec[2], Jerzy Dworak[1], Sebastian Stano[1], Artur Czupryński [3]

[1] Łukasiewicz Research Network – Institute of Welding, Bł. Czesława 16-18, 44-100 Gliwice, Poland
[2] Silesian University of Technology, Division of Engineering Materials, Faculty of Materials Engineering, Krasińskiego 8, 40-019 Katowice, Poland
[3] Silesian University of Technology, Mechanical Engineering Faculty, The Chair of Welding, Konarskiego 18A, 44-100 Gliwice, Poland

Corresponding author: Michał Urbańczyk, michal.urbanczyk@is.lukasiewicz.gov.pl

Abstract: The paper presents the results of structural investigations of a laser-welded layer in the Inconel 625 and Stellite 6 alloy matrix with the addition of WC. The tests involved the use of on plates made of low-alloy steel S355J2C+N. The filler materials used in the tests were nickel-based (Inconel 625) or co-balt-based powders (Stellite 6) having various contents (0-25%) of spherical tung-sten carbide (WC) used as the reinforcing phase. The granularity of the powders was re-stricted within the range of 45 µm to 90 µm. The cladding tests involved making multi-layer overlay welds. Next, non-destructive (VT and PT) and destructive (macro, hardness) tests were carried out. The macroscopic metallographic tests revealed that the three-layer Inconel 625-based overlay welds (with a WC content of up to 15%) had the correct shape and were characterized by full fusion into the base material, ensuring the continuity of the overlay weld.In the case of the Stellite 6-based overlay welds containing 10% of WC, it was possible to observe a through-crack of the overlay welds. The crack was formed in the first layer (as a result of stresses during the solidification of the liquid metal) and developed during the deposition of subsequent layers. The macrostructural tests were supplemented with microstructural observations and microanalysis of the chemical composition (EDS). The above-named tests revealed the good stirring of alloying elements in the overlay weld, indicating the high homogeneity of the overlay weld.The hardness obtained on the surface of the padding weld was 600 HV1.

Key words: cladding; laser metal deposition; LMD; gradient layers; Inconel 625, Stellite 6.

1. INTRODUCTION

Advanced engineering structures and technological processes increasingly often require the use of advanced structural materials and special surface processing methods to ensure the reliability and effective operation of structures [1]. Individual elements of equipment and machinery have to satisfy special requirements, particularly as regards the core and the surface of materials [2]. As can be seen, the surface engineering sector is facing increasingly difficult challenges and must reach out for new tools [3,4]. One of such tools is the laser beam used as the heat source in surface layer processing methods (e.g. surface hardening, alloying or cladding) [5,6].

Laser metal deposition (LMD) enables the very precise deposition of coatings (particularly of thin layers) characterised by only slight dilution, impossible to obtain using conventional cladding methods [7-9]. Laser surface processing may involve very small areas of strictly specified dimensions. It is possible to obtain required properties only in areas where such properties are necessary in terms of tribological or mechanical aspects, because of chemical effect or due to thermal loads. Special LMD methods are used both in the production and repair of poorly accessible structure surfaces [10-11].

It is necessary to perform multi-aspectual research aimed to assess the technical and technological applicability of powder deposition methods and their effect on the structure and properties of overlay welds. The article presents technological and material-related experience gained during the laser metal deposition of gradient layers containing carbides.

Laser deposition is a process where an alloy characterised by specific chemical composition and properties is deposited on surfaces of structural elements. The joining of the material results from the thermal effect of laser beam radiation both on the base material and on the material the overlay weld is made of (Figure 1) [13]. The filler material has the form of a wire (solid or flux-cored) or powder.

The laser deposition method is applied in production processes (deposition of surfaces characterised by special properties (corrosion resistance, abrasive wear resistance, resistance to erosion or cavitation) or to perform repair cladding aimed to reconstruct damaged or worn surfaces [14-17].

One of the advantages of the laser deposition process is the accurate control of a heat input, enabling the precise deposition of coatings and appropriate adjustment of the dilution zone. The above-named advantage enables the making of thin layers characterised by a pre- defined structure [17]. Laser deposition methods are successfully used in the processing of surface layers of e.g. swaging tools, plastic working tools, structures made of sheets/plates or miniature elements characterised by high manufacturing accuracy (where conventional cladding materials (e.g. tools steels) are used) [18,19].

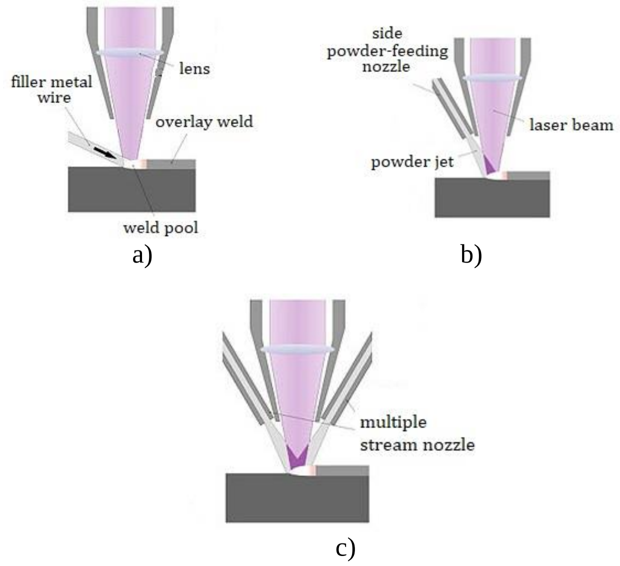

Fig. 1. Variants of the laser deposition process: a) laser deposition with the filler material in the form of a wire, b) laser metal deposition with the side powder-feeding nozzle and c) laser deposition with the multiple stream nozzle

In the laser deposition process the thickness of the dilution layer is restricted within the range of approximately 10μm to 20μm [3], which ensures the obtainment of the appropriate metallurgical joint of the deposited material and the base material. In addition, the application of high heating and cooling rates enables the obtainment of very hard deposited layers [4].

The laser deposition process is characterised by the high precision of the deposition of coatings both on flat surfaces and, e.g. on corners or ribs. As a result, finishing allowance can be small and so can be losses of the deposited material [20, 21].

The laser deposition process can be performed in one or two stages.The one-stage process involves the deposition of the filler material on the layer accompanied by the simultaneous effect of laser beam radiation. In turn, during the two-stage process (also known as the pre-placed technique), the previously deposited (e.g. sprayed) material is melted using the laser beam [8]. The course of the laser deposition process depends on the adjustment of many parameters including, among other things:

• in relation to laser radiation beam and the beam focusing optical system: beam power, radiation wavelength, resonator operation mode (pulsed or continuous), focus location and the shape of the focusing area;

• in relation to powder and its feed system: physicochemical properties, grain size, powder flow (feed) rate, powder flow direction, the type of the carrier gas and its flow rate as well as the shape of the nozzle;

• in relation to an element (substrate) subjected to deposition: deposition rate, physicochemical properties (melting point, linear expansion coefficient, tensile strength, melting point etc.), the position of the substrate in relation to the powder feeding nozzle, the overlap of deposited beads, the number of layers, preheating, etc.

The above-named parameters affect the laser deposition process through interaction taking places in two areas, i.e. laser radiation beam – powder and laser beam – powder - substrate.

The primary laser beam radiation-related parameter affecting the course of technological processes is power density. The power density value typical of the laser deposition process is restricted within the range of 104 to105 W/cm2 [4]. The radiation beam power density is defined by the power of the beam and the size of the focusing area (resulting from the position of the focus in relation to the surface subjected to the deposition process).

The radiation beam power reaching the substrate is lower than the power of the beam leaving the nozzle of the working head. Losses of energy result from the absorption and the scattering of the laser beam by the powder and depend on the time during which the beam affects the powder surface while the powder is transported between the powder feeding nozzle and the surface subjected to deposition. Therefore, losses of beam energy depend, among other things, on the powder flow (feed) rate, the shape and the density of the powder stream as well as the distance between the powder feeding nozzle and the material surface [22, 23]. Powder grains absorb some part of beam radiation energy and melt. The primary stage of the laser metal deposition process is the laser beam-triggered formation of the melt pool (of a previously specified depth) to which molten powder grains are supplied [22]. The interaction between the laser beam transmitted through the cloud of the powder (and reaching the surface of the element subjected to deposition) and the base material is the function of absorption and reflection by the surface subjected to the laser deposition process [23].

The shape and the thickness of the melt pool layer depend on the distribution of beam energy in the focusing area, the powder feed rate and direction, energy transferred by partially melted power grains, the rate of the cladding process as well as the shape of the focusing area [24]. The shape of the beam focusing area (circular, square, rectangular, elliptical, etc.) determines the density of beam radiation power of a given process [20]. The laser metal deposition technology enables the obtainment of precise welds in the form of single layers, the thickness of which is restricted within the range of 0.1 mm to 1 mm [4,7]. The thickness of multi-layer overlay welds can exceed several millimetres. It is possible to perform the cladding process in the macro scale, i.e. involving the elements, the area of which amounts to several square decimetres as well as in the micro scale, i.e. involving precise (e.g. medical) elements, whose wall thickness amounts to 0.1 mm [7].

Another important advantage of the laser deposition process is the possibility of making precise gradient layers or interlayers between the substrate and the surface layer, eliminating the susceptibility of laser deposited overlay welds to cracking [4,5]. In many technological cases it is required that a desirable change in material properties towards a given direction be gradual, smooth and controllable. Such a change ensures the optimum adjustment of a specific structural element to expected operating conditions. The above-named properties can be found in the so-called functionally graded materials (FGM), often referred to as variable functionality materials [25].

Functionally graded materials do not contain the zone characterised by the high gradient of properties, thus sensitive to various imperfections, e.g. transition areas between individual components of a given material. The above-named zone is replaced with an area characterised by gently changing properties, enabling the optimum adjustment of the material to its intended functions and applications [26].

The gradual change in functional or structural properties may take place along various directions. In most applications the aforesaid change occurs across the thickness of a material. The change may be continuous or stepped, affect the entirety of the material or its specific zones (usually in the coating or the transition zone between various components - see Figure 2).

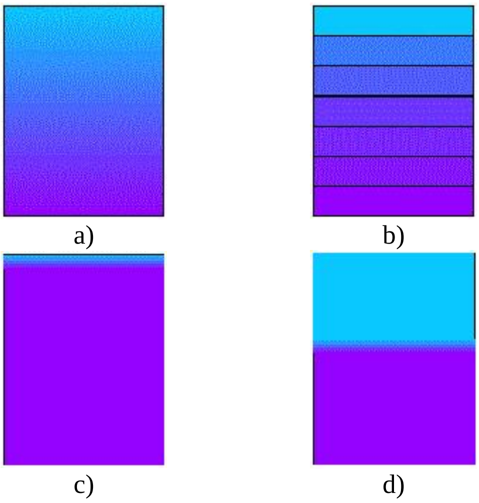

Fig. 2. Schematically presented changes in properties in the volume of a graded material: a) continuous change b) stepped change, c) in the coating and d) in the transition zone

The continuous change can be achieved, for instance, as a result of the continuous change in the content of individual components of a given material across its thickness. In turn, the stepped change requires the use of appropriately selected various materials deposited in layers across the thickness of the material. In terms of the microstructure, the gradient may be concerned with the volume fraction, arrangement, shape and the size of a component (Figure 3).

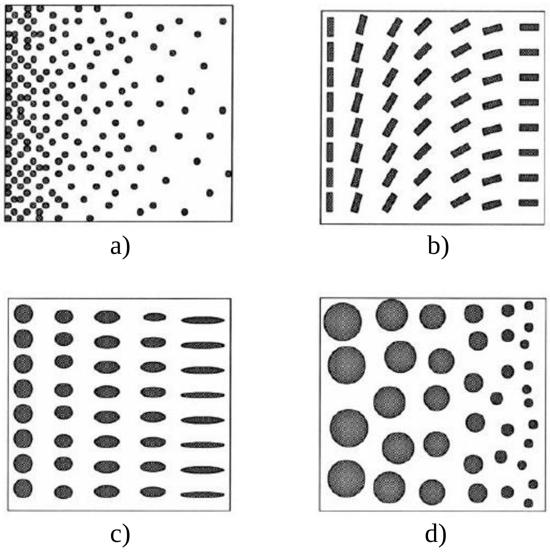

Fig. 3. Gradient of the volume fraction (a), arrangement (b), shape (c) and component size (d) [25]

The hard phase, i.e. carbides, in the overlay weld made using homogenous (single-component) powders is formed as a result of physico-chemical reactions occurring during the surfacing process. The content of the hard phase, affecting the hardness of a deposited layer, results from the amount and types of alloying components of the powder [27-29].

The content of the hard phase in the overlay weld can be increased by performing the process involving the use of two powders (multicomponent powders). Components of one powder form a plastic and metallic matrix containing hard grains (e.g. WC, SiC or TiC compounds having the features of a ceramic material) of the other powder, thus forming composite overlay welds. The hard phase of such powders is not formed solely as a result of physico-chemical reactions taking place during the process of deposition but it constitutes an initial component of multicomponent powders. Frequently, the hard phase component is tungsten carbide. In comparison with other carbides, such as SiC and TiC, tungsten carbide is characterised by combined advantages including high hardness, high density and good wettability by a molten metal [30].

Laser deposition involving the use of multicomponent powders enables the obtainment of deposited layers characterised by complex chemical compositions and properties. This deposition method is becoming increasingly popular when making metal-carbide type complex composite coatings. Traditional techniques applied to this end, e.g. thermal spraying, plasma spraying or arc overlay welding, are characterised by both advantages and disadvantages. Thermal spraying is very efficient, yet it fails to provide the proper adhesion (joint) between the surface layer and the substrate. In turn, arc-based technologies, less effective than thermal spraying, provide a considerable heat input to a material subjected to surfacing, which, in turn, results in significant penetration in the substrate and the substantially greater dilution of the overlay weld material with the substrate. Laser deposition appears to be the most favourable technology as it combines the advantages of both of the above-named methods; it is characterised by the slight dilution of the overlay weld material with the substrate and enables the obtainment of the proper joint (adhesion) of the overlay weld with the substrate. The laser deposition method involving the use of multicomponent powders ensures the effective introduction of hard phase particles, e.g. SiC, TiC and WC carbides to the metallic base, the primary alloying constituents of which are Ni, Co or Fe, and forming ceramic-metallic overlay welds characterised by very high hardness and abrasion resistance. However, the making of such overlay welds entails a number of difficulties and, as a result, has not found many industrial implementations, being restricted to special applications [31,32].

The primary restrictions include cracks in the deposited layer and the low process efficiency. The ormation of cracks in the deposited layer is a complex process affected not only by the thermophysical properties of the substrate and those of the overlay weld material, i.e. a melting point, the coefficient of elasticity and a thermal expansion coefficient, but also process conditions including process parameters, the composition of a metallic base, the content of carbides in the powder mixture and the size of grains in the individual fractions of the powder [31].

Conventional single-layer laser overlay welds made using powder of the specified content of the hard phase and of the matrix can be characterised by inappropriate adhesion or excessively high stresses between the surface layer and the substrate, resulting in the formation of cracks, exfoliation or the chipping of such layers. Cracks (usually initiated) [32] are related to the content of the hard phase in the deposition powder and the resultant significant gradient of physical properties, particularly in the transition zone between the substrate and the overlay weld.

The restriction of the disadvantageous effect of the transition zone as well as the attenuation of the gradient of physical properties can occur in various ways. The slight attenuation of the gradient of properties can take place after the deposition of not one but a few (thinner) layers using powder characterised by the same content of individual components of the matrix and the hard phase (Figure 4). In such a case, a change in properties of the overlay weld is obtained as a result of a slight change in the content of the substrate material and the hard phase in individual layers triggered by the specific degree of dilution with a previous layer.

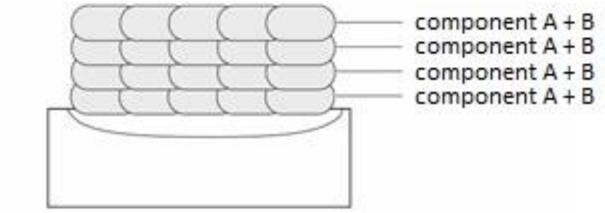

Fig. 4. Schematic structure of the conventional multi-layer overlay weld; each layer is made using powder characterised by the same content of individual components of the matrix and the hard phase

The gradient of changes in properties in the transition zone can be attenuated to a greater extent by making successive layers of the overlay weld using filler metals of various appropriately adjusted chemical compositions (wire or powder – Figure 5(a)) or having the same chemical composition, yet characterised by various contents of components (multicomponent powders) in each subsequently deposited layer (Figure 5(b)).

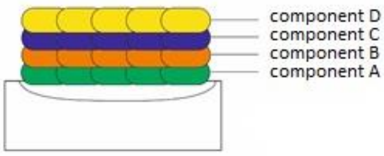

a)

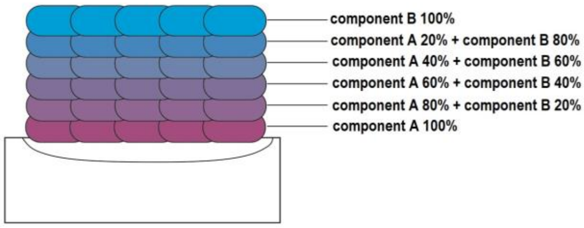

b)

Fig. 5. Schematic structure of exemplary laser-deposited gradient layers a) layer characterised by the stepped change in properties, b) layer characterised by the quasi-continuous change in properties

Gradient layers obtained in the above-presented fashion change their properties in a stepped manner (Figure 5(a)) or uniformly (Figure 5(b)), making it possible to restrict or even eliminate the aforesaid imperfections. The laser powder deposition of typical gradient coatings characterised by the quasi-continuous change in properties (Figure 5(b)) involves the effect of the laser radiation beam on a powder mixture consisting of two components of appropriately adjusted contents of hard carbide particles and ductile metallic matrix in relation to each subsequently deposited layer. Because of the very fast crystallisation of the liquid metal pool, (molten or partly molten) carbide grains are deposited in the plastic matrix.

Usually, gradient layers are characterised by higher hardness and wear resistance than layers applied conventionally and, as a result, significantly extend the service life of machinery elements exposed to complex stresses including abrasion, impact or thermal and mechanical fatigue [33]. Individual layers may be tasked with various roles. Usually, the first layer (made of powder without the hard phase content) is a buffer layer as it bonds well both with the substrate material and with successive layers having specifically adjusted properties. The powder used for the making of next layers is selected as a result of the change in contents of individual phases (base and hard phase) so that the resistance of the surface layer of the workpiece to specific wear in expected operating conditions could be increased. Usually, the surface layer is characterised by higher hardness than that of the base layer.

The search for technologies enabling the production of new compositions of gradient materials focus not so much on the entire form of the material but rather on the obtainment of surface gradient layers on ready-made structural elements. The analysis of available reference publications indicates the possibility of developing new technologies enabling the making of gradient layers characterised by previously specified properties. One of such technologies is the laser metal deposition method (LMD). The article discusses the technological potential, structure and properties of deposited gradient layers having various tungsten carbide contents.

2. MATERIALS AND METHODS

The research-related tests involved the making of one, two and three-layer overlay welds (having a length of 45 mm and a width of 22 mm) on plates made of low-alloy steel S355J2C+N (in accordance with EN 10025-2:2007). The filler materials used in the tests were nickel-based (Inconel 625, Table 1) or cobalt-based powders (Stellite 6, Table 2) having various contents (0-25%) of spherical tungsten carbide (WC) used as the reinforcing phase. The granularity of the powders was restricted within the range of 45 µm to 90 µm. The first layer of the Stellite 6-based overlay weld contained 5%, whereas the second layer contained 7% (by weight) of WC. In turn, the first two layers of the Inconel 625-based overlay weld did not contain any WC additions, whereas the third layer contained 25% (by weight) of tungsten carbide. The use of various tungsten carbide (WC) volume fractions in the individual layers enabled the obtainment of gradient overlay welds characterised by variable properties across the thickness.

Table 1. Chemical composition of the Inconel 625 powder (2.4856) having a granularity restricted within the range of 45 µm to 90 µm

Contents of alloying components [% by weight], according to the certificate				
C	**Si**	**Mn**	**Nb**	**Fe**
0.018	0.370	0.430	3.420	2.780
Cr	**Mo**	**Ti**	**Ni**	
21.370	9.400	0.100	rest	

Table 2. Chemical composition of the Stellite 6 powder having a granularity restricted within the range of 45 µm to 90 µm, according to the certificate

Contents of alloying components [% by weight], according to the certificate					
C	**Co**	**Cr**	**W**	**Si**	**Ni**
0.018	rest	27.700	4.380	1.370	1.540
Fe	**Mn**	**Mo**	**S**	**P**	**B**
1.200	0.100	0.050	0.006	0.01	≤0.005

Technological tests of the laser powder deposition of gradient layers were performed using a robotic station equipped with a KUKA KR30HA industrial robot, a TruDisk 12002 YAG disc laser having a power of 12 kW (TRUMPF) and a specialist deposition head provided with a focusing lens having a focal length of 220 mm. A laser radiation beam was entered into the head using a standard optical fibre having a diameter of 600 µm. The electrically controlled positioning of the head collimator lens enabled automatic changes in a position of the laser beam focus restricted within the range of -4.3 mm to +48.1 mm, thus making it possible to change the area of laser radiation focusing.

The head used in the laser deposition process was provided with an ND16 three-way process nozzle tasked with the formation of the focus of powder jets coaxially in relation to the laser beam. The deposition powder was fed to the process nozzle through the powder distributor made of acrylic. Directly before the nozzle, the distributor homogenised the powder jet and divided it into three single jets entering three channels uniformly arranged around the nozzle circumference. The three jets were situated at a specified angle in relation to the nozzle axis and concentrated 16 mm away from the face surface of the nozzle (Figure 6).

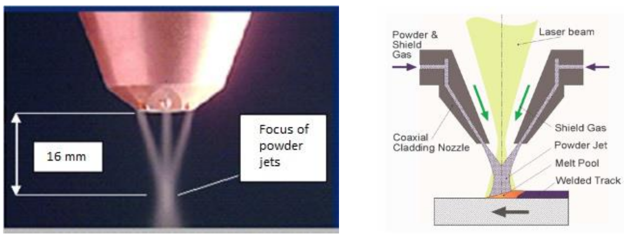

a) b)

Fig. 6. Concentration of powder jets by the three-way nozzle (a) and the schematic diagram of the laser powder deposition process (b) [34]

The amount of transported powder was continuously controlled by adjusting the flow rate of the carrier gas and the revolutions of the disc carrying the powder from the container to the transport conduit.

The previous individual research [22-24] made it possible to determine the position of the laser beam 25 mm away from the powder focusing plane. As a result, an area of laser beam focusing having a diameter of approximately 3 mm was obtained. The adopted welding rate of 1 m/min corresponded to the mean value of a laser deposition rate. It was assumed that the weld width-weld height ratio should be 3:1. The power of the laser radiation beam amounted to 2500 W. The amount of powder fed was identified on the basis of the filling of the overlay weld cross-section of a previously adopted shape (having a width of 3 mm and a height of 1 mm) and the obtainment of a proper single-run overlay weld characterised by the slight dilution with the base material (assuming the above-presented parameters of the deposition process). The above-presented process parameters were used in all of the technological cladding tests. Figure 7 presents the profile and the power distribution of the laser beam used in the tests.

The profile and the power distribution of the laser beam were determined using a Laserscope UFF 100 laser beam analysis device (Prometec).

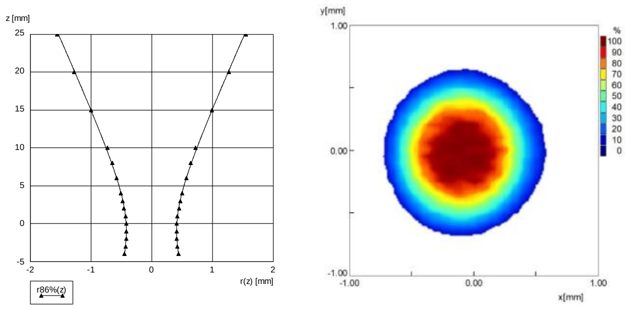

a) b)

Fig. 7. Profile of beam radiation and the size of the focusing area - YAG R laser (86%)=0.509 mm, E (86%) = 4.41x104 W/cm2, tot. mean radius = 0.533 mm, a) 2D graph of the laser beam created on the basis of the measurement of the ray measured in the plane of the x and y axes, calculated in accordance with the PN-EN ISO 11146 standard, b) laser beam power density distribution layered diagram

After the penetrant tests, performed to reveal the presence of cracks (if any), the overlay welds were subjected to metallographic tests. Exemplary macro and microstructures revealed using metallographic specimens and observed using a stereoscopic microscope (Olympus SZX9; dark field observation technique) and a magnification of up to 50x are presented in Figures 8-11. The above-named tests were supplemented with structural observations performed using a scanning electron microscope (SEM) and the microanalysis of the chemical composition performed using the EDS method and a Hitachi S3400N microscope provided with an EDS analyser (Noran). The tests were performed using the secondary electron technique (SE) and the back-scattered electron technique (BSE). The SE imaging enabled the identification of the structure topography, whereas the BSE technique made it possible to determine changes in the chemical composition of individual areas. The observation results concerning the overlay weld structure and the results of the point and linear microanalysis of the chemical composition (EDS) in the fusion area of the three-layer Inconel 625-based overlay weld and of the two-layer Stellite 6-based overlay weld are presented in Figures 12-13. Results of Vickers hardness tests performed using a hardness tester (Struers Abramin) and a load of 9.807 N (HV1) are presented in Figure 17.

3. RESULTS

The analysis of visual test results concerning the faces of the overlay welds made using the LMD process revealed that the application of the assumed process parameters enabled the obtainment of proper overlay welds reinforced with tungsten carbide within the range of 0% to 25% (Figures 8(a)-11(a)).

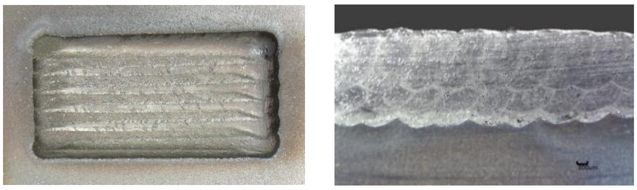

a) b)

Fig. 8. Structure of the three-layer overlay weld: a) face, b) overlay weld macrostructure; substrate – steel S355, overlay weld: 87% Inconel 625, 13% WC

a) b)

Fig. 9. Structure of the three-layer overlay weld: a) face, b) overlay weld macrostructure; substrate – steel S355, overlay weld I: 95% Inconel 625+5% WC, overlay weld II: 90% Inconel 625+10% WC and overlay weld III: 85% Inconel 625+15% WC

a) b)

Fig. 10. Structure of the two-layer overlay weld: a) face after penetrant tests for the presence of microcracks, b) overlay weld macrostructure; substrate – steel S355, overlay weld: 95% Stellite 6 - 5%WC

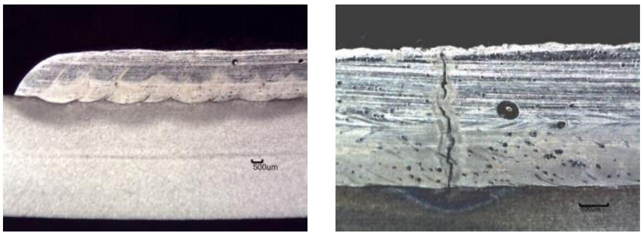

a) b)

Fig. 11. Structure of the two-layer overlay weld: a) overlay weld in the cross-section perpendicular in relation to the direction of surfacing, b) crack revealed in the overlay weld, substrate – steel S355, overlay weld: 90% Stellite 6 - 10%WC

The Inconel 625 alloy-based overlay welds containing up to 25% of tungsten carbide (WC) were made using the LMD method and Vn = 1m/min, beam diameter dog =3 mm and laser power P=2.5 kW. The Stellite 6 alloy-based overlay welds containing up to 10% of WC were made using Vn = 1m/min, beam diameter dog=3 mm and laser power P=2.5 kW. The maximum thickness of the three-layer overlay welds amounted to 4 mm (Figure 9(b), 10(b)), whereas the thickness of the two-layer overlay welds amounted to 2.5 mm (Figure 10(b), 11(b)).

The macrostructural tests revealed the presence of few welding imperfections in the Stellite 6-based overlay weld (primarily pores having a diameter of less than 500 µm) (Figure 11(a)). The Stellite 6-based overlay weld having a 10% addition of WC contained a crack (across the overlay weld (Figure 11(b)). The detailed analysis of the crack trajectory revealed that it was a hot crack. The aforesaid crack was formed in the first layer as a result of stresses accompanying the solidification of liquid metal and developed during the deposition of subsequent layers (Figure 11(b)).

The macrostructure of the remaining overlay welds was proper and characterised by the full penetration in the base material, which ensures the continuity of the overlay weld, particularly when such welds are used as heat-resistant layers exposed to erosive conditions. The tests did not reveal the presence of unmelted grains of the matrix material, which indicated that the course of the LMD process was proper and that the matrix material solidified in the melt pool.

The macrostructural tests were supplemented with microstructural observations and the microanalysis of the chemical composition of phases and structural components. The overlay weld structure contained large spherical particles of tungsten carbide surrounded by the layer of complex carbides in the matrix composed of dendrites and eutectics in the interdendritic spaces (Figure 12(a)). It was also possible to observe large complex carbides in the interdendritic spaces (Figure 12(b)). The microanalysis results concerning the chemical composition of the overlay weld confirmed that the large spherical tungsten carbides were surrounded by the layer of complex carbides containing tungsten, chromium, nickel, molybdenum and iron (Figure 13). The layer of carbides was formed as a result of the partial melting of the WC surface and its reaction with the matrix. This positive phenomenon indicated the formation of the continuous bond of the tungsten carbide and of the matrix.

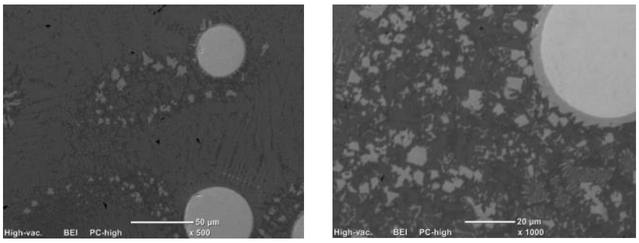

a) b)

Fig. 12. Microstructure of the Inconel 625-based LMD overlay weld: a) structure of the second layer with visible large spherical tungsten carbides with fine carbide precipitates and b) complex carbides in the eutectic areas of the overlay weld

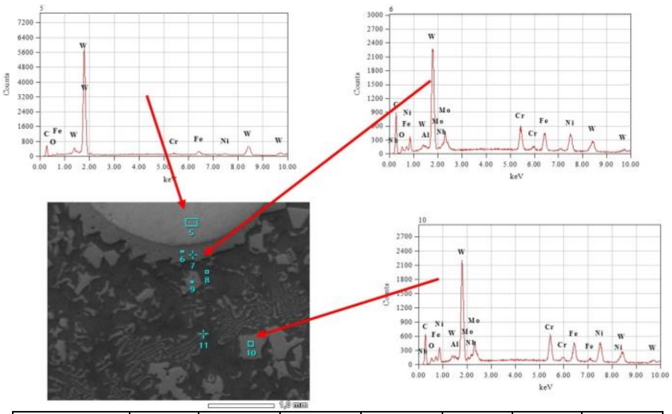

% by weight	Al	Cr	Fe	Ni	Nb	Mo	W
Point 5		0.77	4.45	1.79			92.99
Point 6	0.39	9.74	11.27	16.97	2.61	9.09	49.93
Point 7	0.59	13.5	18.59	37.7		5.67	23.94
Point 8	0.5	14.25	23.16	47.87	0.26	3.21	10.75
Point 9	0.35	11.14	12.06	19.43	2.82	8.77	45.42
Point 10	0.45	10.52	10.97	18.08	2.86	9.38	47.74
Point 11	0.72	16.37	21.4	47.14	1.02	3.91	9.43

Fig. 13. Results of the microanalysis of the chemical composition in the WC-matrix bond area

It was also possible to observe numerous complex carbides formed as a result of the separation of carbides from the WC surface and (within the temperature range of the overlay weld liquid-solid state) their migration to the interdendritic zones (Figure 13). The chemical composition of the aforesaid carbides was similar to that of the complex carbides on the WC surface. The foregoing was also confirmed by the linear distribution of chemical elements in the zone of the bond of spherical WC with the matrix (Figure 14). The line of tungsten distribution clearly revealed a change in the tungsten content in the WC particle (surrounded by the complex carbide and the matrix).

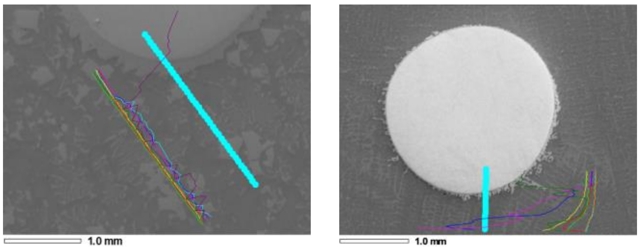

a) b)

Fig. 14. Results of the microanalysis of the chemical composition in the WC-matrix bond area: a) in the Inconel 625-based LMD overlay weld, b) the Stellite 6-based LMD overlay weld

The linear distributions of the surface contents of individual chemical elements (EDS) in the overlay welds (both those based on Inconel 625 and those based on Stellite 6) confirmed the proper stirring of the chemical elements in the overlay welds and, consequently, their significant homogenisation (Figure 15 and 16).

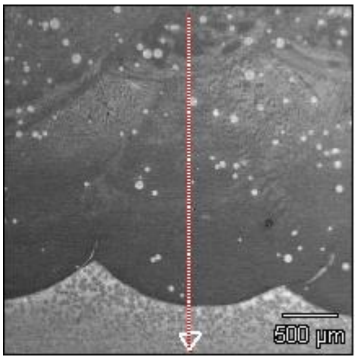

a)

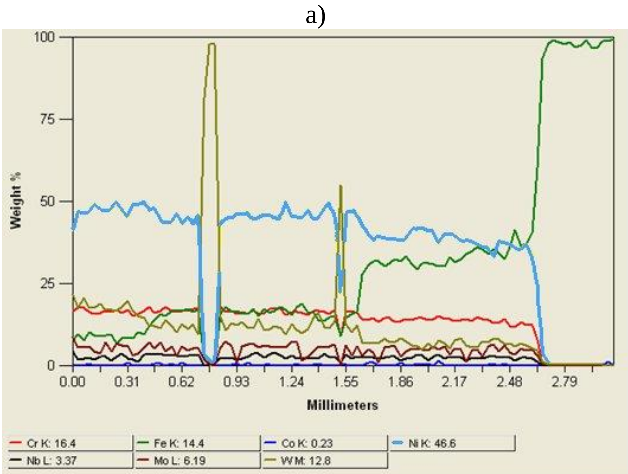

b)

Fig. 15. Results of the microanalysis (EDS) of the chemical composition of the three-layer overlay weld having the matrix of Inconel 625 (95%, 90%, and 85%) with a 5%, 10% and 15% WC addition respectively: a) microstructure and the results of the local analysis of the chemical composition (EDS) and b) results of linear analysis (EDS) on the overlay weld fusion line

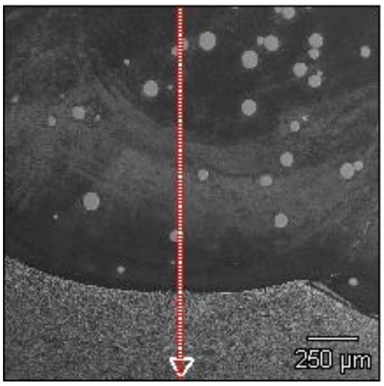

a)

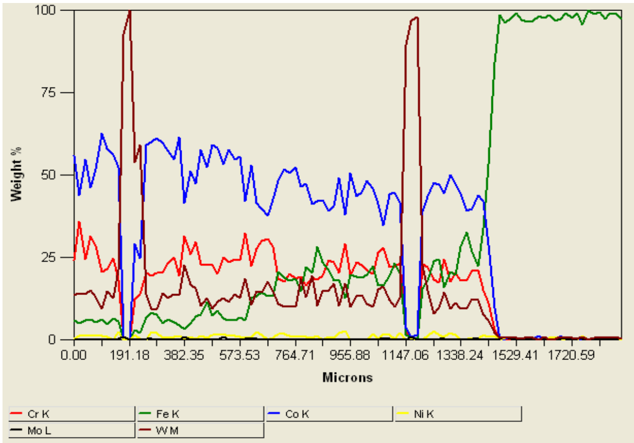

b)

Figure 16. Results of the assessment of the two-layer overlay weld based on the matrix composed of Stellite 6 (95%) and a 5% addition of WC: a) microstructure and the results of the local analysis of the chemical composition (EDS) and b) results of linear analysis (EDS) on the line of the fusion of the overlay weld in the base material

Hardness measurements performed along the vertical line perpendicular to the direction of cladding revealed that the hardness of the last layer of the Inconel 625-based overlay weld was restricted within the range of 600 HV to 470 HV and decreased gradually in the subsequent layers. The foregoing indicated the hardening of the overlay weld and a homogenous increase in hardness (important in terms of internal stresses and further operation, e.g. under high-temperature corrosion conditions and in erosion conditions (Figure 17a).

Similar hardness tests were performed in relation to the Stellite 6-based overlay weld. Also in the above-named case the maximum hardness was detected in the last layer. The hardness of the overlay weld decreased in each previous layer. It was also possible to notice slight surges in hardness between successive layers (Figure 17b).

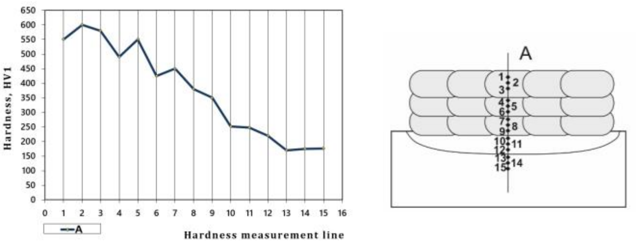

a)

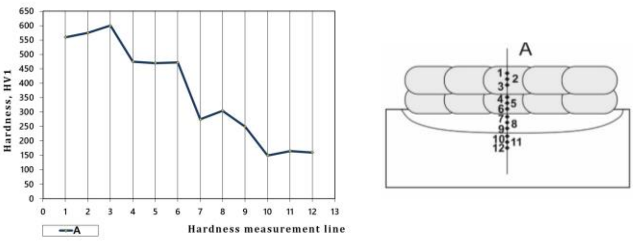

b)

Fig. 17. Results of the microanalysis (EDS) of the chemical composition of the three-layer overlay weld having the matrix of Inconel 625 (95%, 90%, and 85%) with a 5%, 10% and 15% WC addition respectively: a) microstructure and the results of the local analysis of the chemical composition (EDS) and b) results of linear analysis (EDS) on the overlay weld fusion line

4. DISCUSSION

Alloy Inconel 625 is composed of nickel and chromium as well as iron, molybdenum, niobium and other chemical elements. The alloy is characterised by very high corrosion resistance and high temperature resistance (up to approximately 1000°C). As the alloy is resistant to a number of highly corrosive environments, it has found applications in the chemical industry, marine engineering, environmental protection and in the space industry. One of the new technological applications of the alloy involves its deposition on boiler elements such as heat exchanger tubes or membrane walls. This issue is of particular importance as regards systems recovering thermal energy contained in municipal solid waste (incineration plants). Such energy recovery systems constitute an integral part of state-of-the-art systems tasked with the complex management of municipal solid waste. Flue gases emitted during the incineration of such waste contain very aggressive chemical compounds harmful to the environment (e.g. sulphides, chlorides and fluorides). High temperature combined with chemically aggressive flue gas are responsible for high-temperature corrosion. For this reason, boiler elements exposed to the above-named factors must be appropriately protected, particularly by nickel alloys [1]. Recently performed tests involved the application of the laser deposition method to make heat-resistant layers and layers resistant to corrosion [9,10]. The laser metal deposition process involving the use of cobalt-based powders can find applications, among other things, in the refurbishment of various tools exposed to high temperature (e.g. pressure casting moulds, die inserts, hot shears and guillotine shears, elements of presses and moulds for the press forming of light metals, inserts for the formation of plastics, etc.) [22, 24, 30].

The application of the LMD technology makes it possible to precisely control the width of the heat affected zone (HAZ). In the test overlay welds, the HAZ width did not exceed 500 μm, which significantly reduced dilution (Figures 8-11). The aforesaid aspect is particularly important as regards the high-temperature corrosion of elements subjected to the LMD process. An increase in the content of iron on the overlay weld surface above 10% changes the mechanism of corrosion. In contrast with the layer of Cr2O3, the iron oxide formed on the surface is brittle and discontinuous. Results concerning the effect of the content of iron on the susceptibility of Inconel 625-based deposited layers to corrosion are discussed in publication [1]. The technological tests involving the laser metal deposition (LMD) of Inconel 625-based overlay welds revealed that it was possible to obtain such layers and, in addition, to modify them by adding tungsten carbides (Figures 9(a) and 10(a)). The layers obtained in the tests were continuous and free from cracks and other structural discontinuities. The aforesaid imperfections are unacceptable as (in the corrosive environment) they lead to the corrosion of the base material. A tungsten carbide addition of up to 25% significantly improves the resistance of layers to erosive wear, which is of particular importance in terms of protective layers of elements used in biomass incineration plants or in thermal municipal solid waste management plants [1, 2]. The nickel-based three-layer overlay welds contained structures typical of cladding processes, i.e. crystals of the nickel-based structure, building up on partially melted grains of the base material and arranged perpendicularly to the direction of heat discharge (Figures 8(b), 9(b)). The interdendritic areas contained eutectic phases (Figure 12) rich in nickel, chromium, iron, molybdenum and tungsten (Figure 13). It was also possible to observe precipitates of polygonal phases rich in tungsten (Figures 13, point 10), probably composed of chromium, tungsten and molybdenum carbides (Figure 12). In spite of significant dilution in the first layer, the use of the multilayer cladding process limits the content of iron on the overlay weld surface below 1% (which was indicated by the linear distribution of iron in the first layer (Figure 14)). In turn, the linear analysis of the distribution of the remaining chemical elements indicated their high homogeneity, thus providing favourable resistance to

corrosion and erosion (Figure 14). The observations of the overlay weld microstructure revealed that carbide particles were globular, uniform and continuously bonded with the matrix by means of a film rich in tungsten, nickel, chromium and molybdenum (Figure 13). In turn, as regards the multilayer overlay weld made using a filler material characterised by the changeable content of tungsten carbide (up to 25%), the distribution of the aforesaid phase was uniform in the individual layers. The hardness of such a multilayer system increased along with the tungsten carbide content (to 600 HV1) (Figure 17(a)), which implied favourable corrosion resistance. The laser metal deposition process involving the use of cobalt-based powders can find applications, among other things, in the refurbishment of various tools exposed to high temperature (e.g. pressure casting moulds, die inserts, hot shears and guillotine shears, elements of presses and moulds for the press forming of light metals, inserts for the formation of plastics, etc.) [22, 24, 30].
The use of alloy Stellite 6 as the matrix for tungsten carbide grains made it possible to provide the overlay weld with approximately 5% of tungsten carbide and obtain proper (crack-free) overlay welds without the preheating of the base material (Figure 10). The structural tests of the two-layer overlay weld (Stellite 6 -95% + WC -5%) revealed that the fusion area contained a zone of crystals building up perpendicularly to the substrate (Figure 10(b)). On the boundaries of the crystals it was possible to observe eutectic phases rich in chromium (31%), cobalt (38%), tungsten (27%) and iron (approximately 4%). The overlay weld contained spherical precipitates rich in tungsten and eutectic areas surrounding the aforesaid precipitates. The above-named eutectic areas were also rich in tungsten, yet they contained approximately 21% of cobalt and 15% of chromium.
The analysis of the linear distribution of chemical elements in the fusion area indicated that, as regards the Stellite 6-based matrix, the dilution in the first layer of the overlay weld was of lesser importance (Figure 16(b)). The iron content in the first overly weld was below 4%, which enabled the making of proper two-layer overlay welds, providing sufficient resistance to corrosion and erosion. The foregoing was also confirmed by hardness test results revealing that the hardness of the second overlay weld amounted to 600 HV1 (Figure 17(b)). The aforesaid hardness indicates high erosion resistance and the applicability of such overlay welds as abrasion-resistant layers. An increase in the volume fraction of tungsten carbide to 10% resulted in the formation of (relaxation) cracks in the overlay weld structure (Figure 11(b)). The presence of relaxation cracks is only acceptable in abrasion-resistant layers. The use of spherical tungsten carbide in composite powder leads to the obtainment of gradient layers, where the last layer may contain up to 25% of the aforesaid carbide without triggering the formation of cracks and without necessity of preheating the base material. The above-named feature is an important advantage of the laser metal deposition process (LMD), enabling the precise fabrication of gradient layers (of predefined resistance to corrosion or erosion) as well as abrasion-resistant layers.

5. CONCLUSIONS

The tests and the analysis of the test results justified the formulation of the following conclusions:
• The laser deposition technology based on the LMD method makes it possible to obtain multilayer overlay welds based on the Inconel 625 alloy as well as based on the Stellite 6 alloy with an addition of tungsten carbide; • The macroscopic metallographic tests revealed that the three-layer Inconel 625-based overlay welds (with a WC content of up to 15%) had the correct shape and were characterized by full fusion into the base material, ensuring the continuity of the overlay weld. The macroscopic metallographic tests revealed that the three-layer Inconel 625-based overlay welds (with a WC content of up to 15%) had the correct shape and were characterized by full fusion into the base material, ensuring the continuity of the overlay weld; • The microscopic examination of the multilayer overlay welds on the nickel matrix (Inconel 625) revealed structures typical of surfacing processes, i.e. crystals of the nickel-based structures building up on the partly molten grains of the base material, arranged perpendiculary to the direction of heat heat discharge. The interdendritic regions contained eutectic phases rich in nickel, chromium, iron, molybdenum and tungsten; • The use of multilayer overlay cladding ensured that the iron content on the overlay weld surface was less than 1% (Inconel 625), despite the significant stirring of the first layer of the overlay weld with the base material;
• The two-layer overlay welds based on the Stellite 6 alloy were characterised by the uniform structure across the entire cross-section. The dilution (of the matrix material and that of the base) in the first layer was constant and amounted to less than 4% of iron; •
The linear distributions of the surface contents of individual chemical elements (EDS) in the overlay welds, both on the Inconel 625 matrix and on the Stellite 6 matrix, confirmed the good stirring of the alloying elements in the overlay weld and thus indicated the high homogeneity of the overlay weld; •
The hardness distribution tests revealed that the hardness of the last layer of overlay weld both on the matrix of nickel (Inconel 625) and cobalt (Stellite 6) was restricted within the range of 600 HV1 to 470

HV1 and gradually decreased in subsequent layers to 250 HV1.

6. REFERENCES

1.Adamiec J. (2009). *High temperature corrosion of power boiler components cladded with nickel alloys*, Materials Characterization, **60**(10), Elservier Science Inc., pp. 1093-1099

2. Szymański K., Hernas A., Moskal G., Myalska H. (2015). *Thermally sprayed coatings resistant to erosion and corrosion for power plant boilers* A review, Surf. Coat. Technol. vol. **268**, pp. 153-164,

3. Shrestha S. (2002). *Herstellung amorpher etalloberflächenschichtenmittels Laserstrahl*. Dissertation, Technische Universität Berlin, pp. 3-34, Berlin.

4. Dobrzański L. (2009). *Kształtowanie struktury i własności powierzchni materiałów inżynierskich i biomedycznych*, Institute of Engineering Materials and Biomaterials, Silesian University of Technology. pp. 58-94, Gliwice

5. Schubert E., Seefeld T., Rinn A., Sepold G. (1999). *Laser Beam Cladding: A Flexible Tool for Local Surface Treatment and Repair*. Journal of Thermal Spray Technology. **8**(4) December, pp.590-596.

6.Penn W. (2008). *Laser Cladding Basics*. W. Journal, vol. 02. American Welding Society, pp.47-49

7. Information Materials LaserVorm, http:/www.laservorm.com, Accessed: 21/11/2016.

8. Arnold J., Volz R. (1999). *Laser Powder Technology for Cladding and Welding*. Journal of Thermal Spray Technology, **8**(2) June, pp. 243–248

9. *Laser powder coating technology*. Materials of Castolin Eutectic. http://www.castolin.com, Accessed: 10/03/2018.

10. *Laser Metal Deposition*, http://www.trumpf.com. Accessed: 01/06/2018.

11. Nowotny St., Scharek S., Kempe F., Beyer E. (2003). *COAXn: Modular System of Powder Nozzles for Laser Beam Build-Up Welding*. 22nd International Congress on Applications of Lasers & Electro-Optics, P519, pp. 13-16.

12. *Laser Cladding and Additive Manufacturing*. Fruanhofer IWS Dresden. http://www. iws.fraunhofer.de. Accessed: 10/06/2017.

13. Baraniecki T., Chlebus E., Dziatkiewicz M., Reiner J., Wiercioch M. (2011). *System do laserowego mikronapawania proszków metali*. Wroclaw University of Science and Technology, ITMA, Centre of Advanced Production Systems, Welding Review 9/2011, pp. 22-29 .

14. Adamiec J., Łyczkowska K. (2018). *Cracking of pad-welded Inconel 713C precision castings*, Archive of Foundry Engineering. **18**(2), pp. 215-219.

15. *LPW Technology* Ltd. http://www.lpwtechnology.com. Accessed: 10/11/2015

16. Höganäs AB. *Thermal Surfacing. Powder choice with ease*. http://www.serfla.com.br. Accessed: 10/08/2020.

17. Schneider M. (1998). *Laser cladding with powder*. Ph.D. Thesis University of Twente, pp. 21-26, Enschede, The Netherlands

18. Carroll P. (2009). *The Selection and Specification of Powders for Laser Deposition*. LPW Technology Ltd, Complete Laser Cladding Solutions, pp. 1-11.

19. Łyczkowska K., Adamiec J. (2017): *Repair of precision castings made of the Inconel 713C alloy*, Archive of Foundry Engineering. **17**(3), pp. 210-216

20. Nowotny St. (2018). *Beschichten von Magnesiumlegierungen durch Laser-Pulver-Auftragschweißen*. Fraunhofer-Institut für Werkstoff- und Strahltechnik IWS, pp. 110-116, Dresden.

21. Khalid Imran M.,. Masood S. H., Brandt M. (2010). *Influence of Process Parameters in the Direct Metal Deposition of H13 Tool Steel on Copper Alloy Substrate*.World Congress on Engineering 2010 Vol III, June 30 - July 2, pp. 2010-2017, London, UK.

22.Dworak J., Banasik M., Stano S. (2012). *Badania procesu napawania proszkowego wiązką promieniowania laserów YAG i CO2*. Report: Cf-89 (ST-306/12). The Institute of Welding, pp. 72-101, Gliwice.

23. Dworak J., Banasik M., Stano S, Urbańczyk M. (2013). *Badania procesu napawania laserowego z materiałem dodatkowym w postaci proszku i drutu z uwzględnieniem wytwarzania wierzchnich warstw gradientowych*. Report: no. Cf-92 (ST-320/13). The Institute of Welding, pp. 56-78, Gliwice.

24. Dworak J. (2014). *Napawanie laserowe warstw gradientowych*. Bulletin of The Institute of Welding **6**/2014, pp. 22-31, Gliwice.

25. Lee Po. (2013). *Fabrication, Characterization and Modeling of Functionally Graded Materials*. Thesis Ph.D. Columbia University, pp. 2-22, Columbia.

26.Hernik S. (2009). *Projektowanie elementów konstrukcyjnych z materiałów gradientowych*. Thesis Ph. D., Cracow University of Technology, pp. 10-20, Kraków.

27.Lin W.C., Chen C. (2006). *Characteristics of thin surface layers of cobalt-based alloys deposited by laser cladding*. Surface & Coatings Technology vol. **200**, pp. 4557-4563.

28. Choi J., Chang Y. (2005). *Characteristics of laser aided direct metal deposition process for tool steel*. Int. J. Mach. Tools Manuf., **45**(4-5), pp. 597 - 607.

29. Watanabe Y. (2009). *A Novel Fabrication Method for Functionally Graded Materials under Centrifugal Force: The Centrifugal Mixed-Powder*

Method. Open Access. Materials 2009, pp. 1996-1944.
30. Zhou S., Huang Y., Zeng X., Hu Q. (2008). *Microstructure characteristics of Ni-based WC composite coatings by laser induction hybrid rapid cladding*. Materials Science and Engineering, A 480, pp. 564-572.
31. Zhou S., Dai X. (2010). *Laser induction hybrid rapid cladding of WC particles reinforced NiCrBSi composite coatings*. Applied Surface Science. no. 256, pp. 4708-4714.
32. Zhou S., Zeng X., Hu Q., Huang Y. (2008). *Analysis of crack behavior for Ni-based WC composite coatings by laser cladding and crack-free realization*. Applied Surface Science. no. 255, pp. 1646-1653.
33. Myalska H., Moskal G., Szymański K. (2014). *Microstructure and properties of WC-Co coatings, modified by sub-microcrystalline carbides, obtained by different methods of high velocity spray processes*. Surface & Coatings Technology. vol. **260**, pp. 303-309,
34. Groth A., Walz C., Naegeler S. (2002). *New Innovations in Diode Laser Cladding*. Fraunhofer USA - Center for Surface and Laser Processing, ICALEO 2002, Plymouth, Michigan, USA.
35. Laser cladding. https://www.gtv-mbh.de/en/processes/laser-cladding.html Accessed: 10/06/2016.

Received: March 15, 2022 / Accepted: June 15, 2022 / Paper available online: June 20, 2022